http://dx.doi.org/10.5012/bkcs.2011.32.11.4099

Sintering Behavior of Copper Nanoparticles

En-Kyul Yu, Longhai Piao,* and Sang-Ho Kim*

Department of Chemistry, Kongju National University, Chungnam 314-701, Korea
**E-mail: piaolh@kongju.ac.kr (L. Piao), sangho1130@kongju.ac.kr (S.-H. Kim)*
Received April 30, 2011, Accepted September 16, 2011

Key Words : Printed electronics, Copper nanoparticles, Oxidation, Conductivity

Printed electronics, in contrast to conventional vacuum deposition- and lithography-based patterning methods, provide direct-written patterns on substrates with common printing equipments, such as screen, flexography, gravure, offset lithography and inkjet printers.[1-3] The establishment of such low-cost graphic printing techniques has facilitated the development of affordable electronics for a variety of applications, including flexible displays, smart labels and animated posters.[4,5] Printed electronics combines materials, printing equipment and process technologies. Electrically functional materials, such as metal nanoparticles,[6] semiconductor nanomaterials,[7] polymers,[3,8] and carbon nanotubes,[9] are employed in printable electronics. These materials can be printed onto a substrate, to create active or passive devices, such as conducting electrodes, thin film transistors and resistors.

Silver nanoparticles are used most frequently as printable conducting materials on account of their high electrical conductivity and chemical stability.[10,11] However, their price hinders their commercialization. Therefore, the development of a low-cost printing material that can replace silver for the printing of conducting patterns is important for the advancement of printed electronics.[12,13] Among various candidate materials, copper is promising due to its high electrical conductivity and low price. However, in order to employ copper as a printable electrode material, there exists one huge problem to be solved: the oxidation of copper during the sintering process.[12] Common approaches to circumvent this involve the direct sintering of Cu powders under oxygen-free or reductive environments to prevent significant oxidation.[14,15] Recently, Jang *et al*. reported the sintering of inkjet-printed Cu nanoparticles on a flexible polyimide substrate.[16] They obtained Cu patterns with high conductivity by sintering Cu nanoparticles in formic acid. However, the details of oxidation and reduction during sintering were unclear. Systemic study of the chemical changes of Cu nanoparticles during sintering would aid the understanding of this complex and important reaction. This work reports an examination of the sintering behavior of Cu nanoparticles by varying temperature, time and environment.

Figure 1 shows scanning electron microscopy (SEM) and transmission electron microscopy (TEM) images of the Cu nanoparticles used in this study. The nanoparticles (*ca*. 25 nm) were synthesized by reducing Cu(II) acetylacetonate with 1,2-hexadecanediol.[17] Oleic acid and oleyl amine were introduced as capping agents during synthesis, facilitating the dispersal of the nanoparticles in non-polar solvent. Cu nanoparticles in toluene were coated on to a clean slide glass and dried at ambient temperature for several minutes. After drying, the film was red-brown (Figure 2(a)). Its thickness was *ca.* 10 μm. The films were heat treated in a glove box under various environments. Morphological and structural changes were monitored at various heating temperatures and times.

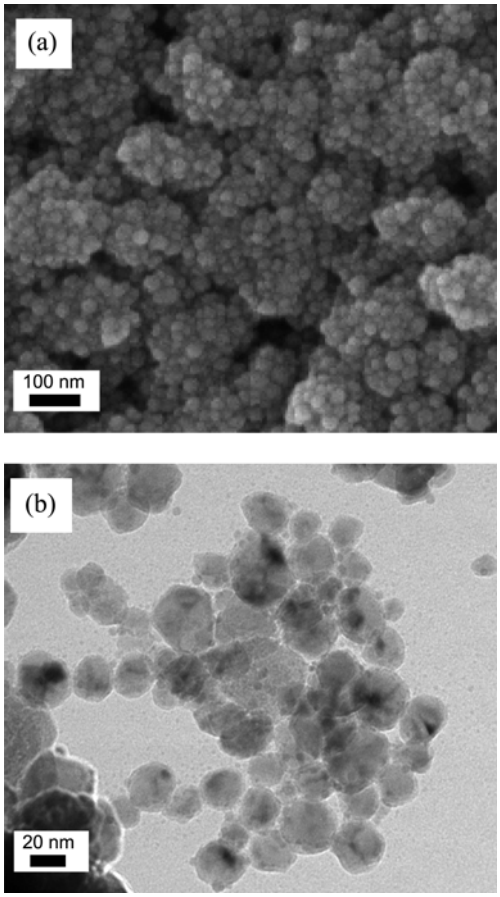

Figure 1. (a) SEM and (b) TEM images of Cu nanoparticles. The scale bars indicate 20 nm.

After heat treatment, the film's color changed depending on the conditions. When heated under air and nitrogen, it became dark green (Figure 2(b) and 2(c)), implying oxidation of the copper. The film heated under formic acid

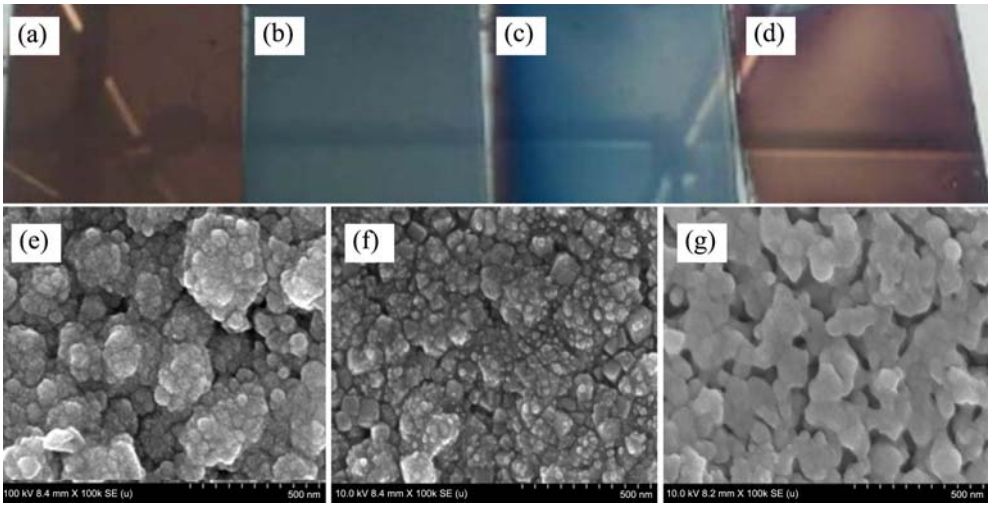

Figure 2. Photographs of the Cu films (a) before and after heat treatment under (b) air (c) nitrogen and (d) formic acid. SEM images of the Cu films heated in (e) air, (f) nitrogen and (g) formic acid.

remained red-brown, indicative of the Cu nanoparticles remaining metallic (Figure 2(d)). Figures 2(e)-2(g) show SEM images of the Cu nanoaprticle films after heat treatment. Their morphologies were also different under the different environment. The Cu nanoparticles heated under air and nitrogen exhibited simple aggregation, not fused networks (Figures 2(e) and 2(f)). Similar to the color changes, this may be attributable to the simple aggregation of oxidized nanoparticles due to its high melting temperatures. The nanoparticles treated in formic acid showed surfaces that had merged with each other, creating a network (Figure 2(g)).

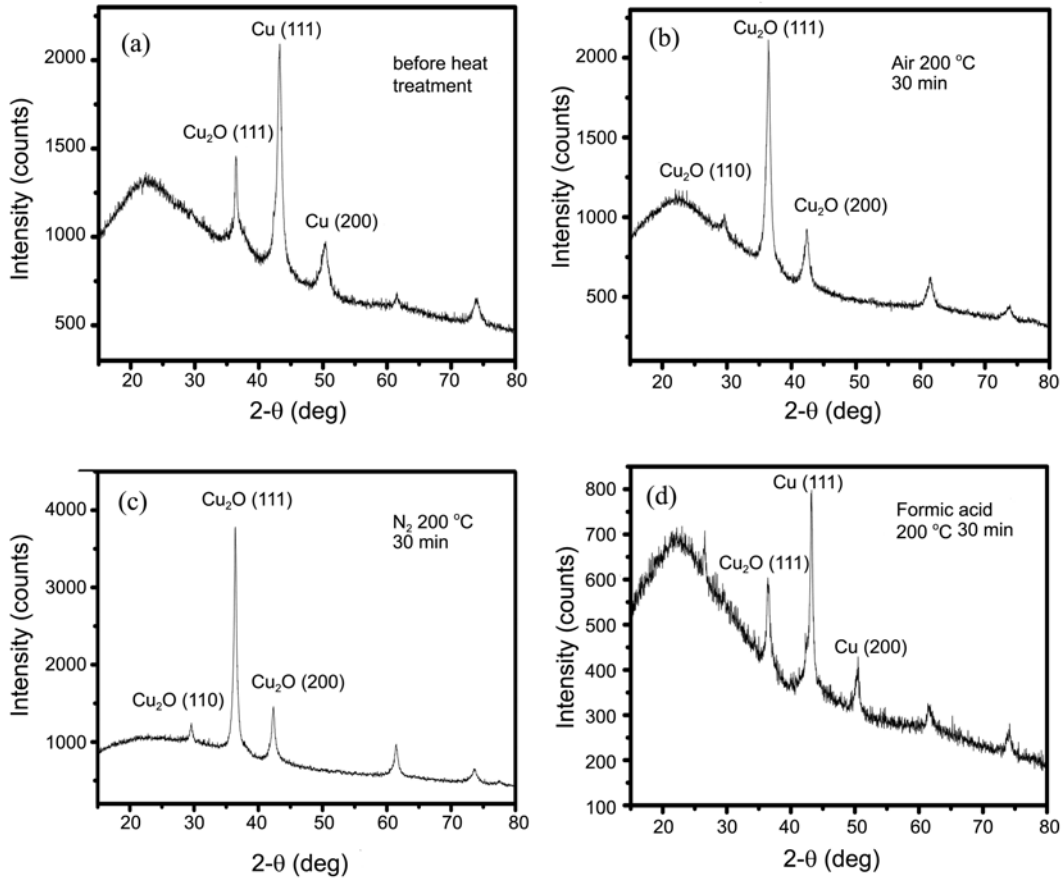

Figure 3. XRD patterns of the Cu films (a) before and after heat treatment under (b) air (c) nitrogen and (d) formic acid for 15 min.

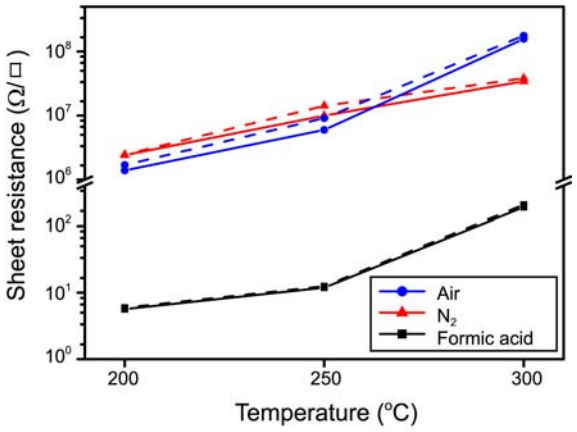

Figure 4. Resistances of the Cu films heated under various environments, temperature and time (15 min, solid line; 30 min, dashed line).

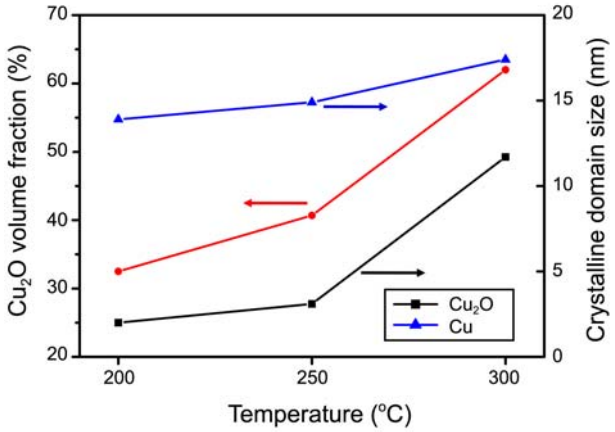

Figure 5. The influence of sintering temperature for the Cu_2O volume fraction, Cu and Cu_2O crystalline domain size of the Cu films heated in formic acid.

To confirm the oxidation of the nanoparticles during heat treatment, the films' crystalline structures were characterized by X-ray diffraction (XRD) analysis (Figure 3). Pristine Cu film showed peaks of the characteristic (111), (200) and (220) planes of face-centered cubic copper (Figure 3(a)). After heat treatment under air and nitrogen, almost all the Cu crystalline peaks disappeared, with only characteristic Cu_2O crystalline peaks observed, indicating that all the Cu nanoparticles were oxidized to Cu_2O (Figures 3(b) and 3(c)). The sample heated under formic acid showed both Cu metal crystal peaks and Cu_2O peaks, suggesting partial oxidation of the Cu nanoparticles (Figure 3(d)).

The films' resistances were compared (Figure 4) to assess the effects of oxidation during heat treatment on electrical conductivity. The films sintered under air and nitrogen showed very high resistance, despite the latter being heated under nitrogen of extremely high purity. The Cu films sintered in formic acid showed resistances as low as several Ω. The lowest resistance of 5.66 Ω/ was observed in the sample sintered at 200 ºC for 15 min. Resistances under all conditions increased with increased sintering temperature, whereas the duration of sintering had negligible effect. In general, nanoparticles' surface melting and sintering are accelerated at higher temperatures and longer duration. Therefore, better conducting networks should be formed at higher temperatures. However, this behavior is reversed for Cu nanoparticles, imputable to the oxidation of the copper.

The influence of oxidation on electrical conductivity was quantitatively analyzed by measuring the crystallinity and crystalline structures of the Cu and Cu_2O under formic acid (Figure 5). The volume fraction of Cu_2O, calculated from the area ratios of the crystalline peaks, increased with increasing sintering temperature, suggesting that oxidation was accelerated at higher temperature. The increase of resistance at high temperature could be attributed to the enhanced oxidation.

The half width of the crystalline peak in the XRD pattern reflects the crystalline domain size of the crystal. Therefore, measuring changes of the crystalline domain sizes of Cu and Cu_2O allows monitoring of particle merging and the competition of oxidation and reduction reactions of the Cu during sintering. Crystalline domain size was calculated from the corresponding half-width of the reflection peak using the Scherrer equation (eq. 1):

$$\text{domain size} = \lambda/(\beta\cos\theta) \quad (1)$$

where λ is the wavelength of the X-rays (1.54 Å for CuKα radiation), β is the half-width of the Cu (111) and Cu_2O (111) peak in radians and θ is the peak position.

As expected, the samples sintered in air and nitrogen had Cu_2O crystalline domains that increased with increasing sintering temperature, indicative of increased oxidation (Supporting Information). The Cu films treated under formic acid had Cu crystalline domains that also increased with increasing sintering temperature due to the melting and merging of the nanoparticles. However, the Cu_2O crystalline domains increased more vastly when the temperatures was higher than 200 ºC (Figure 5). Therefore, at higher temperatures, the rate of oxidation was greater than the rate of reduction and resistances increased significantly.

These results show that Cu, especially when as nanoparticles, is easily oxidized even by traces of oxygen. This prevented the direct sintering of Cu nanoparticles under a high-purity inert atmosphere. Therefore, a combination of inert gas and reducing agent is required to prepare conducting Cu electrodes. Formic acid was used here, as it is economic, of low toxicity and has suitable vapor pressure. The proposed reduction reaction mechanism is summarized in Eq. (2).[16]

$$Cu_2O + HCO_2H(g) \rightarrow 2Cu + H_2O(g) + CO_2(g) \quad (2)$$

The Cu films sintered under formic acid had electrical conductivity determined by competition between melting, oxidation and reduction of the Cu nanoparticles. The optimum temperature was found to 200 ºC, sufficiently high to allow the melting of the 25 nm nanoparticles' surfaces to create a conducting network. At higher temperatures, oxidation was faster than reduction and resistance increased. At

below 200 ºC, for example 160 ºC, resistance was also high due to insufficient decomposition and evaporation of the surfactants. The use of specially designed surfactant that can decompose and evaporate at low temperatures could lower the resistance of Cu electrodes.

In summary, the sintering behavior of Cu nanoparticles was examined by varying the temperature, duration and environment. Severe oxidation was occurred in samples sintered in air and nitrogen, resulting in high resistances. The samples sintered under formic acid had resistances as low as several Ω that increased with increasing sintering temperature. The relationship between resistance and oxidation was quantitatively analyzed by determining crystallinity and crystalline domain sizes by XRD. Increased rate of oxidation compared with reduction by formic acid was responsible for the degradation of electrical conductivity.

Experimental Section

Materials and Methods. Cu nanoparticles of average diameter *ca*. 25 nm were synthesized by reported methods.[17] The sizes and shapes of nanoparticles and films were investigated by a Hitachi (Japan) S-4800 field-emission SEM, and a FEI (Netherlands) Tecnai G2 F30 S-Twin field-emission TEM operating at 300 keV. Samples' crystal structures were characterized by a Micro-Area X-ray diffractometer (D/MAX-2500(18 kW)). Resistance was measured using conventional 4-terminal measurement on a probe station.

Preparation of Cu Films and Sintering. The Cu nanoparticles were dispersed in toluene using a homogenizer. The Cu nanoparticle film was prepared by coating the toluene solution of Cu nanoparticles on a clean slide glass with a wire bar. Sintering was performed in a glove box on a hotplate under flows of air, nitrogen (99.99%) and formic acid vapor at 200, 250 and 300 ºC for 15 and 30 min.

Supporting Information Available. Table S1, Cu_2O crystalline domain sizes under air and nitrogen environment.

Acknowledgments. This research was supported by the grant from the Fundamental R&D Program for Technology of World Premier Materials funded by the Ministry of Knowledge Economy, Republic of Korea, and the National Nuclear R&D Program through the National Research Foundation of Korea (NRF) funded by MEST (20100028702).

References

1. Caironi, M.; Gili, E.; Sakanoue, T.; Cheng, X.; Sirringhaus, H. *ACS Nano* **2010**, *4*, 1451.
2. Sele, C. W.; von Werne, T.; Friend, R. H.; Sirringhaus, H. *Adv. Mater.* **2005**, *17*, 997.
3. Creagh, L. T.; Mcdonald, M. *MRS Bull.* **2003**, *28*, 807.
4. Sirringhaus, H.; Kawase, T.; Friend, R. H.; Shimoda, T.; Inbasekaran, M.; Wu, W.; Woo, E. P. *Science* **2000**, *290*, 2123.
5. Kraus, R.; Malaquin, L.; Schmid, H.; Riess, W.; Spencer, N. D.; Wolf, H. *Nature Nanotech.* **2007**, *2*, 570.
6. Huang, D.; Liao, F.; Molesa, S.; Redinger, D.; Subramanian, V. *J. Electrochem. Soc.* **2003**, *150*, G412.
7. Ahn, J.-H.; Kim, H.-S.; Lee, K. J.; Jeon, S.; Kang, S. J.; Sun, Y.; Nuzzo, R. G.; Rogers, J. A. *Science* **2006**, *314*, 1754.
8. Stutzmann, N.; Friend, R. H.; Sirringhaus, H. *Science* **2003**, *299*, 1881.
9. Hou, Z.; Cai, B.; Liu, H.; Xu, D. *Carbon* **2008**, *46*, 405.
10. Gamerith, S.; Klug, A.; Scheiber, H.; Scherf, U.; Moderegger, E.; List, E. J. W. *Adv. Funct. Mater.* **2007**, *17*, 3111.
11. Smith, P. J.; Shin, D.-Y.; Stringer, J. E.; Derby, B.; Reis, N. *J. Mater. Sci.* **2006**, *41*, 4153.
12. Platzman, I.; Brener, R.; Haick, H.; Tannenbaum, R. *J. Phys. Chem. C* **2008**, *112*, 1101.
13. Luechinger, N. A.; Athanassiou, E. K.; Stark, W. J. *Nanotechnology* **2008**, *19*, 445201.
14. Jeong, S.; Woo, K.; Kim, D.; Lim, S.; Kim, J. S.; Shin, H.; Xia, Y.; Moon, J. *Adv. Funct. Mater.* **2008**, *18*, 679.
15. Wu, S.; Ding, X. *IEEE Trans. Adv. Pack.* **2007**, *30*, 434.
16. Jang, S.; Seo, Y.; Choi, J.; Kim, T.; Cho, J.; Kim, S.; Kim, D. *Scr. Mater.* **2010**, *62*, 258.
17. Mott, D.; Galkowski, J.; Wang, L.; Luo, J.; Zhong, C. J. *Langmuir* **2007**, *23*, 5740.